OUT-OF-PLANE SEISMIC PERFORMANCE OF UNREINFORCED MASONRY WALLS RETROFITTED WITH UNBONDED POST-TENSIONING TENDONS

Daniel Lazzarini[1], Peter Laursen[2], and Cole McDaniel[3]

ABSTRACT

Unreinforced masonry (URM) structures have historically been regarded as structurally unsound in response to seismic events. Retrofit of URM walls in particular is necessary in order to prevent brittle out-of-plane collapse.

A new out-of-plane retrofit design for a URM wall was verified through structural testing. The selected retrofit technique incorporates vertical coring of URM walls to allow for the insertion of single unbonded post-tensioning (PT) tendons spaced at a regular interval. Tensioning of PT tendons increases the strength of the wall and allows it to behave in a ductile manner in response to out-of-plane seismic demands. Mortar mix designs were generated and tested such that a mix could be selected to best reflect the target 80-year-old structures in San Luis Obispo, CA.

An unreinforced masonry wall using vintage brick from the 1920s was constructed in the testing lab. The wall was subjected to cyclic, pseudo-static out-of-plane loading. Testing confirmed that unbonded post-tensioning tendons can be successfully implemented in URM walls to resist out-of-plane loading. Testing showed significant increase of flexural strength and the accommodation of large out-of-plane displacements without collapse. The unbonded PT tendon remained elastic throughout testing and therefore provided a restoring force to the wall returning it to the original alignment after each displacement cycle.

Introduction

This research focused on the retrofit of slender unreinforced masonry (URM) clay brick walls with unbonded post-tensioning (PT) tendons to sustain out-of-plane seismic loading. URM walls are historically associated with brittle collapse and loss of human life. Many URM collapses have resulted from URM wall strength being compromised in out-of-plane bending. These problems associated with this form of construction have been well documented and studied since the 1933 Long Beach earthquake (Campi 1989 and Kariotis and Nghiem 1993). Slender walls are particularly susceptible to out-of-plane collapse, and are categorized by table A1-B of the 2006 IEBC for regions of high seismicity as having a height-to-thickness (*h/t*) larger than 13.

[1] Architectural Engineering Graduate Student, California Polytechnic State University, San Luis Obispo, CA
[2] Professor, Architectural Engineering Dept., California Polytechnic State University, San Luis Obispo, CA
[3] Professor, Architectural Engineering Dept., California Polytechnic State University, San Luis Obispo, CA

This retrofit scheme consists of cavities less than one inch in diameter that are cored vertically down the wall at a regular spacing. After tendons are inserted in the wall, they are anchored and then tensioned using a stressing jack. Tendons are considered unbonded, and are therefore not grouted in place. The presence of unbonded PT tendons and the associated axial force improves the out-of-plane flexural strength of the wall. The unbonded PT tendons are designed to remain elastic, thus providing a restoring force returning the wall to its original position upon unloading.

Retrofit Wall Configuration in the Considered URM Building

Figure 1 shows the retrofit scheme for a typical URM wall. The existing wall is vertically cored at the center ($d_y/2$) at a spacing s. A single unbonded PT tendon is placed in each core (a) and a small cavity is created at the lower diaphragm to allow for the assemblage of the PT anchorage and bearing plate (b). Similarly, at the top of the wall, a cavity can either be created to house the stressing end of the PT anchorage or the tendon can be anchored at the top of the wall parapet (c). After tendon stressing by means of a hydraulic jack, the previously removed bricks can be reinserted to preserve the structure façade.

The unreinforced masonry wall considered in this project is reflective of a wall located in a typical one-story structure situated in San Luis Obispo, California. The wall may either be situated on a concrete spread footing or a brick stem-wall. A typical wall span between diaphragms ranges from 10 to 14 feet. The wall is typically located on the longitudinal face of the structure perpendicular to the street, and has no crosswalls. The two-wythe wall specimen incorporates a running bond pattern with bond courses every sixth course.

Figure 1 (d) shows a generalized configuration of the URM structure considered in this project. In Figure 1 (e), the wall is shown removed from the structure with the location of PT tendons indicated by vertical arrows. The area tributary to one PT tendon is hatched. This area is extruded from the wall in Figure 1 (f) and represents the segment of the wall that was designed and tested (also see Figure 2).

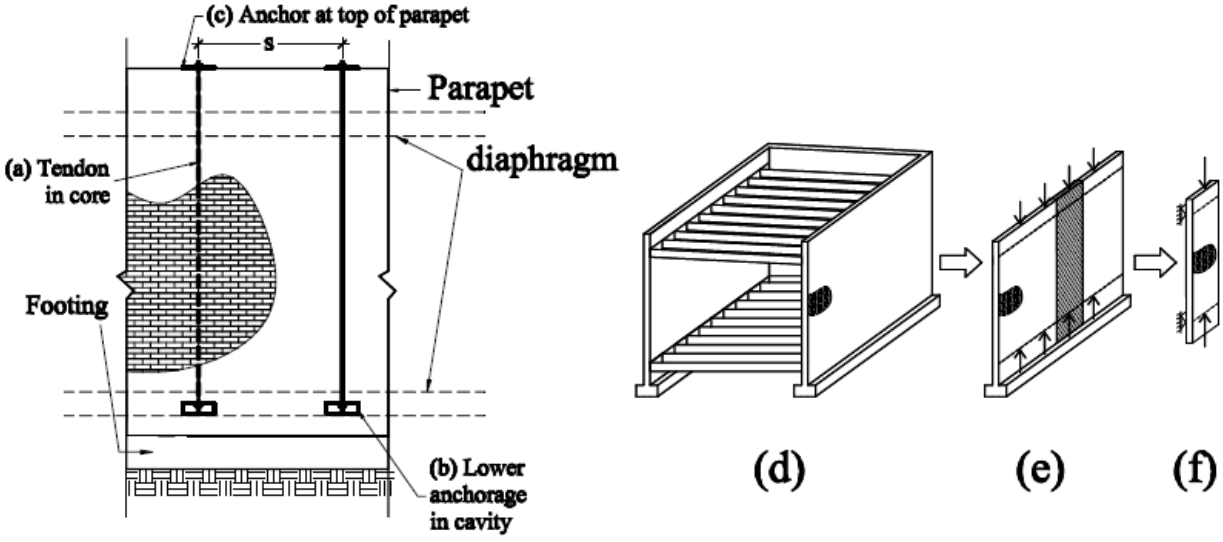

Figure 1: Retrofitted URM Wall Configuration

Material Properties

The red-clay bricks used in this research came from a demolished warehouse that was located in San Jose, CA, and built in the 1920's. Iterations were conducted with regard to mortar mix to achieve a 28-day compressive strength comparable to the strength of an 80-year-old URM wall. A mix design was selected once f'_m entered the established range of 800 psi to 1300 psi (5.5MPa to 9.0MPa) (ASTM C-1314). Specimens for tensile bond strength of masonry f_r were tested in accordance with ASTM C-1072. A final mix design using proportions of 1 : 1 : 9 cement : lime : sand was used. This mix resulted in an average masonry prism compressive strength f'_m = 1,262 psi (8.70MPa) and a tensile bond strength of f_r = 41 psi (0.28MPa). Additional masonry properties such as modulus of elasticity E_m and shear strength V_m are calculated empirically based on the 2005 MSJC Section 1.8 and Section 3.2, respectively. These values are grouped with f'_m, f_r and post-tensioning steel properties in Table 1.

The post-tensioning tendon used in this project was a standard ½" (13mm) diameter, 270 ksi (1860 MPa) tensile strength 7-wire strand conforming to ASTM A416. Standard high-strength steel barrel anchors and wedges were used to transfer the prestress force to the wall.

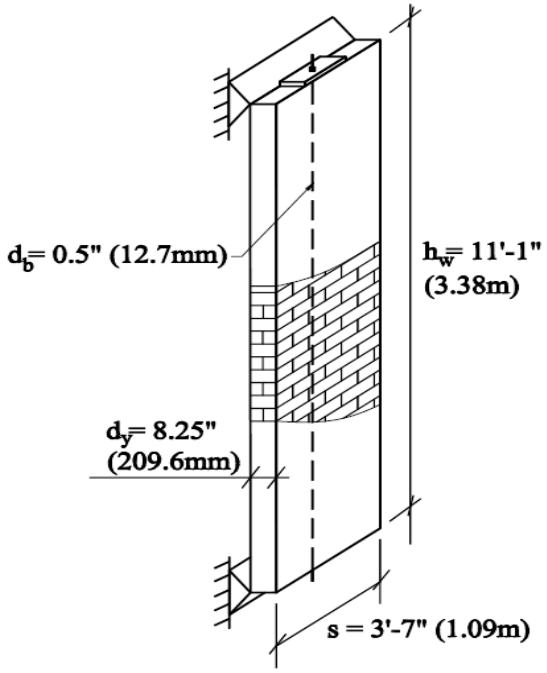

Figure 2: Test Wall Dimensions

Material Properties	
γ lb/ft^3 (kg/m^3)	140 (2,240)
f'_m psi (MPa)	1,262 (8.7)
f_r psi (MPa)	41 (0.28)
V_m psi (MPa)	88.8 (0.61)
E_m ksi (GPa)	883 (6.1)
f_{pu} ksi (MPa)	270 (1,860)
E_s ksi (GPa)	28,500 (197)

Table 1: Material Properties

Proposed Tendon Anchorage Detail

Due to variability in the foundation conditions of URM walls, different post-tensioning anchorage solutions may be necessary in this retrofit scheme. Figure 3 illustrates potential anchorage configurations.

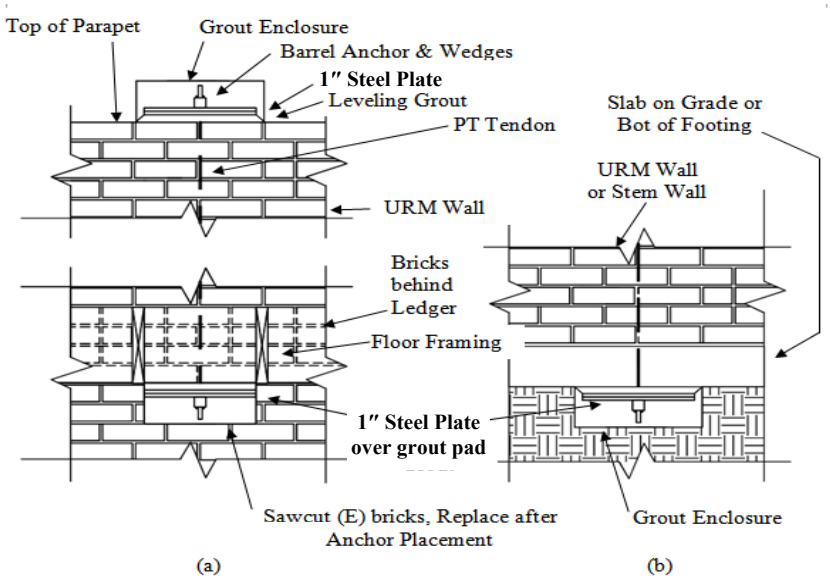

Figure 3: Retrofit Anchorage Details

Option (a) in Figure 3 represents an anchorage solution for a wall that is to be restrained at its lower diaphragm. In this configuration, bricks are removed at the location where the steel plating is inserted. A steel bearing plate is placed on a non-shrink grout pad to allow for spreading of the concentrated PT force. The PT tendon itself anchors to the steel plate by means of a barrel anchor and wedges. After the tendon is tensioned, the cavity can be grouted closed and/or bricks can be trimmed and put back into their original position. The retrofit configuration shown in Figure 3 (b) presents an option for retrofitting a wall that sits on a concrete footing.

Seismic Demands and Predictions for Prototype Wall

The seismic demand was based on a structure located in downtown San Luis Obispo, CA and was generated to assess the performance of the URM wall and the PT retrofitted wall in response to out-of-plane loading (see Table 2). C_s was generated using the Equivalent Static Force procedure in ASCE 7-05 (IBC 2006). Notation is defined at the end of this paper. The URM wall prior to retrofit did not have sufficient strength to resist the design-level ground motion demands. The table also reveals that the retrofitted wall was predicted to withstand the design-level demands while remaining uncracked. The wall was assumed to have pinned supports and uniform distributed load. No strength reduction factors were considered in order to compare predictions to test results. Further details may be found in Lazzarini (2009).

Seismic Demand		**Test Predictions**	
C_s g	0.432	M_{cr} pre-retrofit lb-ft (kN-m)	1,874 (2.54)
w_u lb/ft (kN/m)	148 (2.18)	M_{cr} retrofit lb-ft (kN-m)	4,228 (5.73)
M_u lb-ft (kN-m)	2,240 (3.04)	M_n retrofit lb-ft (kN-m)	6,620 (8.98)
$V_{u\ base}$ lb (kN)	1,628 (7.24)		

Table 2: Seismic Demand and Capacity Predictions

Wall Out-of-Plane Testing

The thickness of the wall throughout was about one brick length. The pin-pin height of the tested wall was 11′-1/2″ (3.38m). These dimensions correlated to a wall height-to-thickness ratio h / t of 18 which is considered slender by the 2006 IEBC. The initial amount of prestress after immediate losses was 50% of the tendon strength, or a tendon force P_{ps} = 20.5 k (91.2kN). The testing program of this project parallels existing studies (Al-Manaseer 1987, Bean et al. 2007, Krause et al. 1996, and Shultz et al. 2004). This project is unique because it incorporated vintage materials and focused on the retrofit of existing URM walls. Existing research has previously only considered new materials and new construction for similar out-of-plane tests on post-tensioned masonry walls. In lieu of coring the wall after construction, the wall was built around the post-tensioning tendon. The tendon was placed inside a flexible conduit roughly ¾" in diameter. The conduit and tendon were hung vertically, made plumb and affixed to the scaffold. Bricks were cut as necessary so that they could be fit around the conduit and tendon.

The testing apparatus was designed so that four equal magnitude point loads could be applied to the wall in the out-of-plane direction to simulate a uniformly distributed load. The test setup and data acquisition system is illustrated in Figure 4.

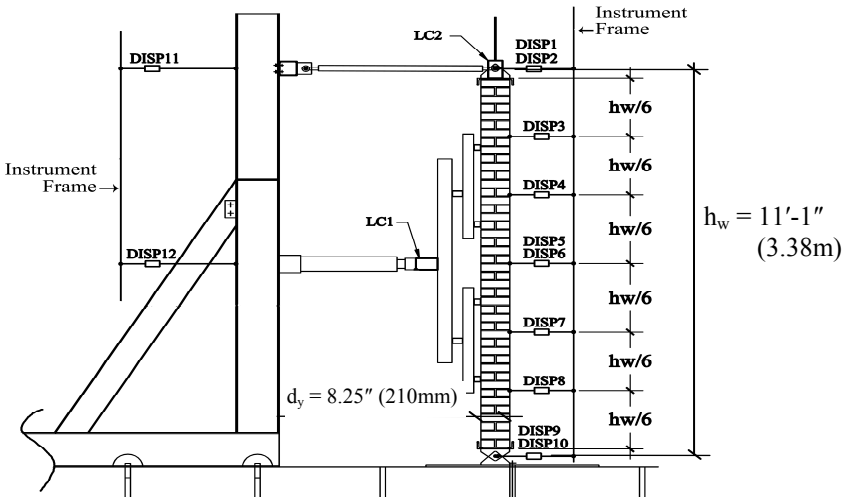

Figure 4: Instrumentation Diagram Side Elevation

Load was applied monotonically in the push direction through a hydraulic ram bolted to the reaction frame. Load was recorded through a load cell placed on the end of the hydraulic ram in contact with the load spreader. The loading apparatus was constructed to allow for pivoting of the individual load points. By doing this, loading remained equal between the four point loads as the wall experienced large deformations. An additional load cell LC2 was located between the tendon anchorage and the top of the wall and monitored the force in the post-tensioning tendon. Displacement transducers were located at the sixth-points on the tension face of the wall. Multiple data sets were recorded within each load cycle. Loading and unloading cycles were both captured in the force-displacement plot. The loading protocol may be referenced in Lazzarini (2009).

Test Results

A force-displacement plot including every displacement cycle is shown in Figure 5. The drift of the wall corresponds to the maximum displacement of the wall relative to h_w.

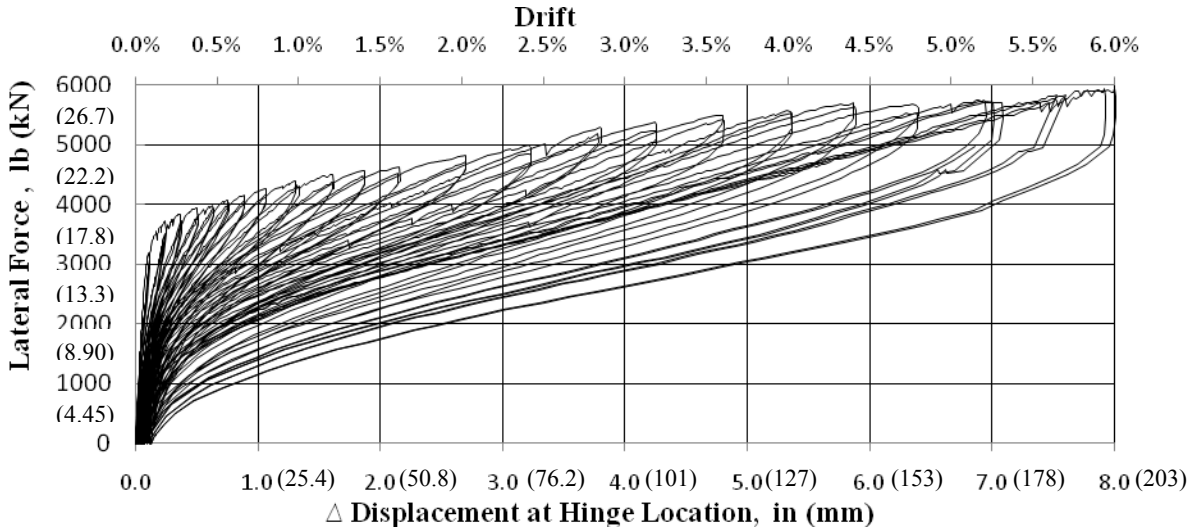

Figure 5: Force-Displacement Response for All Cycles

Figure 6 presents the overall backbone curve for the retrofitted wall. This plot compares the response of the tested wall to predictions based on a four equal-magnitude point load model (predictions and seismic demand shown as dashed lines). The location of hinging in the wall did not occur at mid-height as expected. The hinge formed 3 courses (9″, or 203mm) above the center of the wall. It is the displacement at this hinge location that is plotted in Figures 5 and 6.

As predicted, the wall exhibited twice the strength required to resist the force associated with the design-level ground motion while remaining elastic.

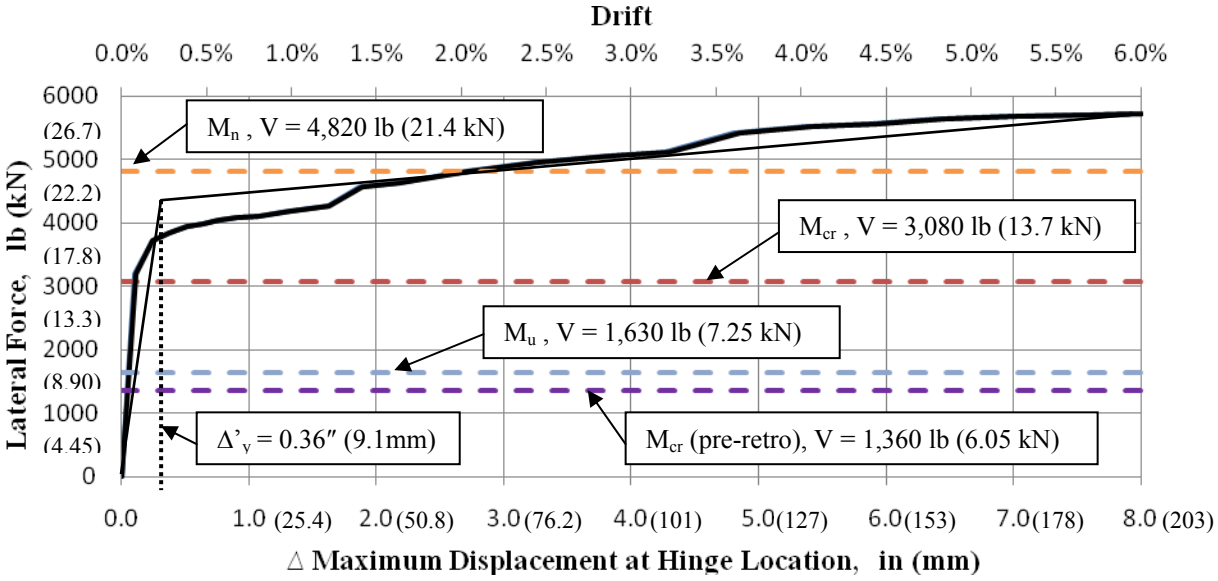

Figure 6: Force–Displacement Backbone Plot

A bi-linear force-displacement approximation is shown in Figure 6 with the intention of finding the pseudo-yield displacement $\Delta'_y = 0.36''$ (9.1mm). The phrase pseudo-yield is used to describe the displacement associated with the formation of the hinge within the wall. This displacement is not a true yield displacement since the PT tendon remains elastic at all times (Lazzarini 2009). If displacement ductility is considered to be the ratio of ultimate displacement (7.960″ or 202mm) to pseudo-yield displacement, the retrofitted wall sustained an out-of-plane ductility demand of $\mu = 22$. Such a high level of ductility is significant because a ductile system is preferred in response to seismic events because it ensures a gradual, rather than an abrupt and catastrophic failure.

The predicted cracking moment capacity compares favorably with the results from the test. Around this point, the wall loses significant stiffness and begins to displace large amounts with relatively smaller additions of load. The wall resisted a moment twice as large in magnitude as that associated with the design-level ground motion. At these force levels, the displacement of the wall was not significant; however, separation of mortar from bricks at the hinge location was visible. Up until the theoretical point of hinging, the displaced shape of the wall was generally parabolic. Once hinging occurred, the displaced shape of the wall reflected the rotation of two rigid bodies hinging about one point.

As evident in the force-displacements plots, the wall was able to achieve large displacements without compromising the masonry's strength. Maximum displacements of almost 8″ (203mm) were achieved, with the wall returning to nearly its initial position after unloading. Figures 7 (a) and (b) show the wall at $\Delta = 3.5''$ (88.9mm) and $\Delta = 8.0''$ (203mm) of displacement. A plumb line was hung on the tension face of the wall to better observe the drift the wall experienced relative to its original alignment. The ultimate displacement the wall achieved was limited to the range of the hydraulic loading ram. At the maximum displacement, the ram was fully extended.

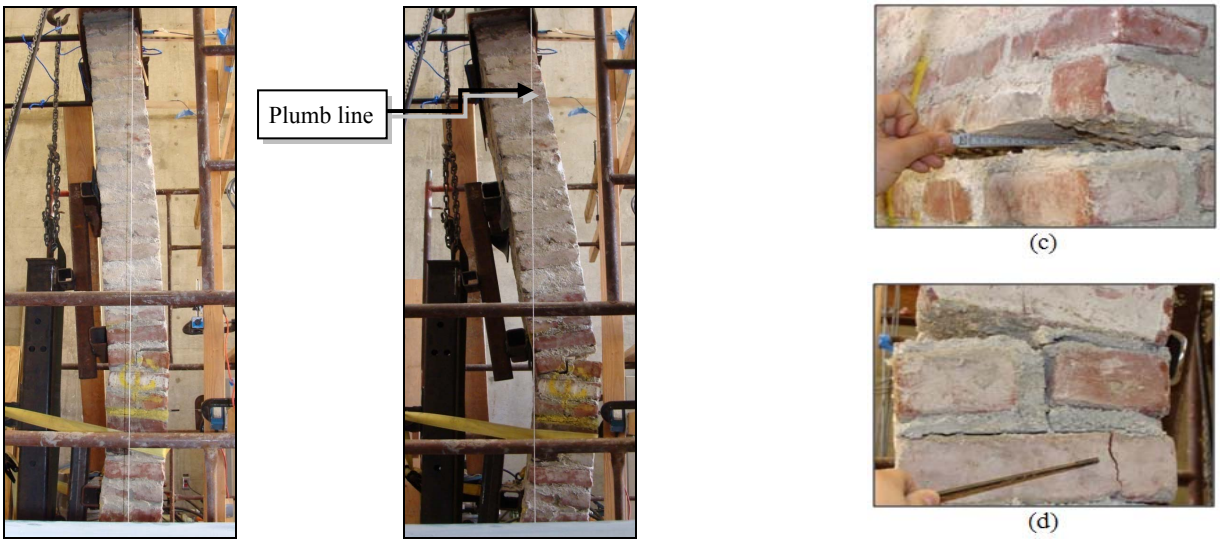

(a) $\Delta = 3.5''$ (88.9mm) (b) $\Delta = 8.0''$ (203mm)

Figure 7: Hinge Displacement

Figure 7 (c) shows the size of cracking at Δ = 8.0″ (203mm), and Figure 7 (d) shows the extent of masonry splitting at the location of the hinge. As a reference, the crack gauge in Figure 7 (c) measures a maximum crack of 0.6″ (15mm).

Ultimately, the wall was able to withstand approximately three times the design load. At high force demands, significant crushing was experienced in the mortar and the brick. This demonstrates a substantial strength increase provided by the addition of unbonded PT tendons. In the region of the Force-Displacement plot beyond cracking, the strength of the wall is controlled by increasing axial forces in the tendon and increasing compressive strains in the masonry at the location of plastic hinging.

Figure 8 shows the change in the tendon force with increasing displacement over all displacement cycles. After the tendon came in direct contact with the wall at approximately Δ = 0.125″ (3.18mm), the stress increased approximately linearly with an increase of displacement.

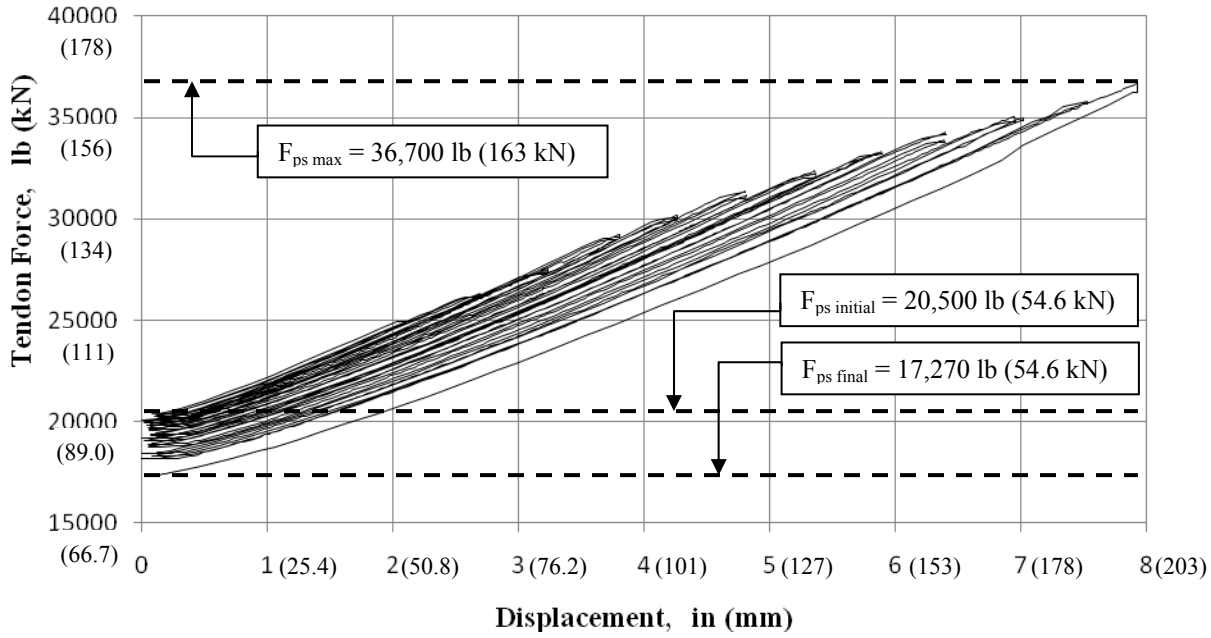

Figure 8: Tendon Force vs. Wall Displacement for all Cycles

The elongation in the tendon at the maximum wall displacement was found to be 0.495″ (12.6mm). Because the tendon is unbonded, the elongation is spread out over the entire length, thus keeping the tendon in its elastic range. It can also be seen that the tendon lost some of its initial force after testing concluded. This is due to the masonry crushing at the hinge region of the wall at high displacement levels. Enough material had undergone inelastic deformation that the wall itself shortened, causing the tendon to slacken. Based on the tendon force loss (16% loss), it was found that the wall had shortened 0.1″ (2.5mm) after the last test cycle. Despite this crushing, the elastic, unbonded PT tendon returned the wall to its original position upon unloading. Similar results have been documented in previous testing (Bean et al. 2007, Krause et al. 1996, Laursen 2002, and Schultz et al. 2004).

The retrofit detail previously shown in Figure 3 was implemented in the test wall (after out-of-plane testing had completed) to demonstrate the validity of the anchorage system under sustained load from the PT tendon (Figure 9). Bricks were removed from the wall and the anchorage shown in Figure 3(a) was created using a 16″x8″x1″ (406mm x 203mm x 25mm) steel plate. The post tensioning tendon was stressed to 90% of its rupture strength (37.2 kips or 166 kN) and the wall was monitored over a period of 14 days. The anchorage system and the wall were able to withstand this force without any noticeable cracking or local damage.

(a) (b)

Figure 9: Post Tensioning Anchorage Test (a) Location in Wall, (b) Anchorage Close-up

Conclusions

Testing demonstrated that a vintage clay brick URM wall retrofitted with unbonded PT tendons can meet and exceed the out-of-plane force demands resulting from the design-level ground motion. This research differs from existing work on post-tensioned masonry walls because it investigates the effects of post-tensioning introduced to existing URM walls in the form of a structural retrofit. In this fashion, vintage bricks from the 1920's were used, and mortar was designed to reflect mortar existing in 80-year-old URM structures located in San Luis Obispo, CA.

Testing not only demonstrated the significant improvement in out-of-plane strength that this system offers URM walls, but also showed that such a system can sustain large out-of-plane displacements while avoiding major residual deformation and damage. Testing also demonstrated the relative ease of assembling and implementing such a system within an existing URM wall. The implementation of this retrofit technique is visibly much less invasive than traditional URM retrofit techniques.

Results of testing show that an unbonded PT retrofit for out-of-plane loads improves wall flexural strength, ultimate displacement capacity, and ductility. It is important to ensure that after a significant increase in PT force, the tendon would remain elastic. It is apparent that if tendon yielding were to occur the system would experience residual displacements and thus, greater post-earthquake damage. Since the restoring force provided by the tendon remaining elastic is strongly desired, design must ensure that the increase in tendon force at a given target displacement does not exceed the yield strength of the tendon.

Notation

A_{ps}	area of prestressing steel, in^2	h_w	effective height of wall, in
C_s	base shear coefficient generated using ASCE 7-05 Equivalent Static Force Procedure, g	M_{cr}	nominal cracking moment strength, in-lb
		M_n	nominal moment strength, in-lb
d_b	tendon diameter, in	M_u	demand moment, in-lb
d_y	wall thickness, in	P_{ps}	prestressing tendon force at time and location relevant to design, lb
E_m	modulus of elasticity of masonry, psi		
E_s	modulus of elasticity of steel, psi	s	spacing of reinforcing or prestressing tendons, in
f'_m	specified compressive strength of masonry, psi	V_m	shear strength provided by masonry, psi
f_{ps}	stress in prestressing tendon at nominal strength, psi	V_u	shear demand, lb
f_r	calculated tensile strength of masonry bond, psi	w_u	out-of-plane uniformly distributed load, lb/in
f_{pu}	specified strength of prestressing tendon, psi	γ	density of URM wall, lb/ft^3

References

Al-Manaseer, A. and V. Neis. "Load Tests on Post-Tensioned Masonry Wall Panels." *ACI Structural Journal.* 84.3 (1987) 467-472.

ASTM C1072: *Standard Test Method for Measurement of Masonry Flexural Bond Strength*, American Society for Testing and Materials, 2006.

ASTM C1314: *Standard Test Method for Compressive Strength of Masonry Prisms*, American Society for Testing and Materials, 2007.

Bean Popehn, Jennifer R., Arturo E. Schultz and Christopher R. Drake. "Behavior of Slender Posttensioned Masonry Walls Under Transverse Loading." *Journal of Structural Engineering*. 133.11 (2007) 1541-1550.

Campi, Dominic E. "Seismic Strengthening of a Historic Unreinforced Masonry Building." *Engineering: Research and Practice.* 1-5 May, 1989, San Francisco, CA., American Society of Civil Engineers, 1989.

FEMA-547: *Techniques for the Seismic Rehabilitation of Existing Buildings*, Federal Emergency Management Agency, United States, 2006.

IEBC: 2006 *International Existing Building Code*, International Code Council, 2006.

Kariotis, John and Doc Nghiem. "In-Situ Determination of the Compressive Stress-Strain Relationship of Multi-Wythe Brick Masonry." *Structural Engineering in Natural Hazards Mitigation: Proceedings of Papers Presented at the Structures Congress*. April 19-21, Irvine, CA, United States. Structural Division of the American Society of Civil Engineers. 1993

Krause, Gary L., Ravi Devalapura and Maher K. Tadros. "Testing of Prestressed Clay-Brick Walls." *Proceedings of the 1996 CCMS of the ASCE Symposium in Conjunction with Structures Congress XIV*. 15-18 April, 1996, Chicago, IL, United States. American Society of Civil Engineers, 1996.

Laursen, Peter T. *Seismic Analysis and Design of Post-Tensioned Concrete Masonry Walls*. Department of Civil and Environmental Engineering, University of Auckland, N.Z. 2002.

Lazzarini, Daniel L. "Seismic Performance of Unreinforced Masonry Walls Retrofitted with Post-Tensioning Tendons." *California Polytechnic State University Digital Commons*, San Luis Obispo, CA. 2009.

MSJC: *Building Code Requirements for Masonry Structures and Specification for Masonry Structures,* ACI 530-05/ASCE 5-05/TMS 402-05, Masonry Standards Joint Committee, United States, 2005.

Schultz, A. E., J. R. Bean and C.R. Drake. "Flexural Behavior of Slender Post-Tensioned Masonry Walls." *Proceedings of the 2004 Structures Congress – Building on the Past: Securing the Future*. 22-26 May, 2004, Nashville TN, United States.